

images is defined by the inner edge of the ring system and/or the effects of the ring shadow, and this is shown clearly in Fig. 2. The 7.8- $\mu\text{m}$  equatorial belt is parallel to the occulting inner edge of the ring system, although uncertainties of up to  $3^\circ$  in tilt and  $5^\circ$  in displacement with respect to the rotational equator cannot be excluded because of latitude structure in the belt. The position of the equatorial emission belt is therefore not inconsistent with the latitude of the magnetic-dip equator<sup>12</sup> at  $6^\circ$  N. The Earth exhibits thermospheric emission in the form of two bright belts of 130-nm atomic-oxygen emission near the magnetic Equator, associated with electron-density enhancements (the Appleton anomalies)<sup>13</sup>. The Earth also has a strong electric current (the equatorial electrojet) flowing east-west along the magnetic Equator and only a few degrees of latitude in width<sup>14</sup>. A similar current system may exist on Saturn, and electron collisional excitation could contribute to the 7.8- $\mu\text{m}$  methane vibrational emission observed. Other effects associated with Saturn's rings could be significant, including convective transport of atmospheric gas to high altitudes along a sharp temperature discontinuity at the inner edge of the ring shadow. Such convective transport could lead to enhanced stratospheric temperatures by ortho-para  $\text{H}_2$  conversion<sup>15</sup>. More exotic processes, such as deposition of material from the rings, cannot be excluded and will be considered as part of a subsequent program of more detailed thermal infrared observations.  $\square$

Received 19 July; accepted 19 October 1989.

1. Gillett, F. C. & Orton, G. S. *Astrophys. J.* **195**, L47-L49 (1975).
2. Rieke, G. H. *Icarus* **26**, 37-44 (1975).
3. Tokunaga, A. T., Caldwell, J., Gillett, F. C. & Nolt, I. G. *Icarus* **36**, 216-222 (1978).
4. Cess, R. D. & Caldwell, J. *Icarus* **38**, 349-357 (1979).
5. Bezard, B. & Gautier, D. *Icarus* **61**, 296-310 (1985).
6. Hanel, R. *et al. Science* **212**, 192-200 (1981).
7. Hanel, R. *et al. Science* **215**, 544-548 (1982).
8. Bezard, B., Gautier, D. & Conrath, B. *Icarus* **60**, 274-288 (1984).
9. Caldwell, J., Halthore, R., Orton, G. & West, R. *Bull. Am. astr. Soc.* **18**, 789 (1986).
10. Gezari, D. Y., Foltz, W. C., Woods, L. A. & Wooldridge, J. B. *Proc. Soc. Photo-Optical Instrum. Engrs* **973**, 287-298 (1988).
11. Deming, D. *et al. Astrophys. J.* **343**, 456 (1989).
12. Connerney, J. E. P. *Geophys. Res. Lett.* **13**, 773-776 (1986).
13. Carruthers, G. R. & Page, T. *J. geophys. Res.* **81**, 483-496 (1976).
14. Hanson, W. B. & Carlson, H. C. in *The Upper Atmosphere and Magnetosphere* 84-101 (Natl Acad. Sci., Washington, DC, 1977).
15. Conrath, B. J. & Gierasch, P. J. *Icarus* **57**, 184-204 (1984).

ACKNOWLEDGEMENTS. The NASA Infrared Telescope Facility is operated by the University of Hawaii under contract from the National Aeronautics and Space Administration.

## Self-organized criticality in the 'Game of Life'

Per Bak, Kan Chen & Michael Creutz

Department of Physics, Brookhaven National Laboratory, Upton, New York 11973, USA

THE 'Game of Life'<sup>1,2</sup> is a cellular automaton, that is, a lattice system in which the state of each lattice point is determined by local rules. It simulates, by means of a simple algorithm, the dynamical evolution of a society of living organisms. Despite its simplicity, the complex dynamics of the game are poorly understood. Previous interest in 'Life' has focused on the generation of complexity in local configurations; indeed, the system has been suggested to mimic aspects of the emergence of complexity in nature<sup>1,2</sup>. Here we adopt a different approach, by using concepts of statistical mechanics to study the system's long-time and large-scale behaviour. We show that local configurations in the 'Game of Life' self-organize into a critical state. Such self-organized criticality provides a general mechanism for the emergence of scale-free structures<sup>3-5</sup>, with possible applications to earthquakes<sup>6,7</sup>, cosmology<sup>8</sup>, turbulence<sup>9</sup>, biology and economics<sup>10</sup>. By contrast to these previous studies, where a local quantity was conserved, 'Life' has no local conservation laws and therefore

represents a new type of universality class for self-organized criticality. This refutes speculations that self-organized criticality is a consequence of local conservation<sup>11</sup>, and supports its relevance to the natural phenomena above, as these do not involve any locally conserved quantities. The scaling is universal in the sense that the exponents that characterize correlation functions do not depend on details of the local rules.

The grand and general question is how the laws of physics—which describe processes on the microscopic scale—can lead to a world organized on all scales. The idea of 'self-organized' is that it is in the nature of nonlinear processes to organize mathematical systems into structures that have order on all length scales. If this tendency is generally present in such mathematical systems, then we would also expect the natural world to contain structures on all scales. Here we demonstrate this by choosing 'at random' an entirely local algorithm, the 'Game of Life', and showing that the model evolves to a stationary state where small perturbations create objects of all sizes.

The canonical example of self-organized criticality is a 'pile of sand'. Imagine building the pile by slowly adding particles. As the pile grows, there will be bigger and bigger avalanches. Eventually a statistically stationary state is reached in which avalanches of all sizes occur, that is, the correlation length is infinite. Thus, in analogy with equilibrium thermodynamical systems the state is 'critical'. It is also self-organized because no fine-tuning of external fields was needed to take the system to the critical state: the criticality is unavoidable. This is in contrast to the behaviour for an equilibrium phase transition,

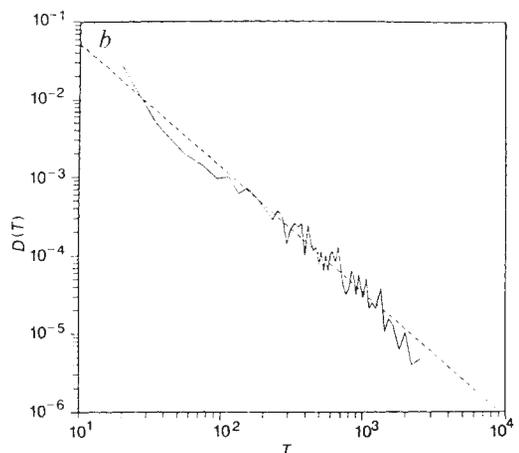
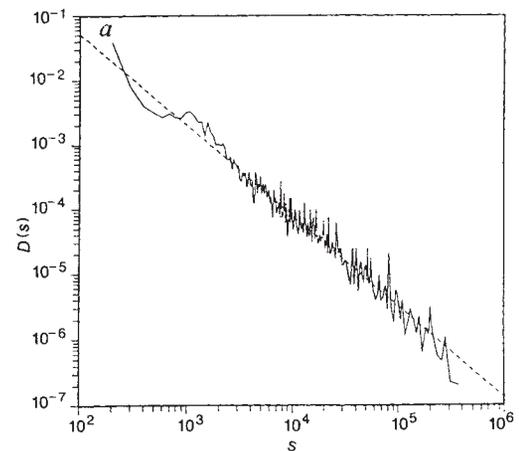


FIG. 1 a, Log-log plot of distribution of cluster size for a  $100 \times 100$  system. b, Distribution of the duration for evolution of clusters. The deviation from power-law behaviour for large clusters is a finite-size effect.

in which one has to tune, for instance, the temperature to arrive at the critical point.

The 'Game of Life' is defined on a square lattice. There are two states on each lattice site, representing the presence or absence of a live individual. The rules for the evolution of 'Life' are very simple. (1) The fate of a live individual depends on its eight nearest neighbours; it will die at the next time step if there are less than two (over-exposure) or more than three (over-crowding) live neighbours; otherwise it will remain alive. (2) At a dead site, a new individual will be born at the next time step only if there are exactly three live neighbours. Figure 2 includes some configurations of still life, cyclic life and propagating gliders. Numerous local stationary configurations can be generated by these simple rules, representing variety and complexity of local stable societies. We will focus, however, on the collective behaviour of live organisms.

We simulate 'Life' on finite lattices of sizes up to  $150 \times 150$ . Open (absorbing) boundary conditions are generally chosen, but the scaling region of the spatial and temporal correlations is not affected by boundary conditions. Of course, the finite size of the system cuts off very-large-scale features. We studied the following process. Starting with a random distribution of live sites, the system evolves according to rules (1) and (2) until it comes to 'rest' in a simple periodic state with a distribution of local still life and simple cyclic life (with our method of generation, cyclic structures of long period are extremely rare and essentially never encountered). The system is then perturbed on a randomly chosen local site, by adding a live individual, and is then allowed to evolve according to the rules until it comes to rest again. As the process is repeated, the system evolves into a statistically stationary state, which does not depend on the initial configuration. The properties of this state are the object of our investigation.

First, we measure the total activity  $s$ , defined as the total number of births and deaths following a single perturbation. Figure 1a shows the distribution of 'clusters' of size  $s$  averaged over 40,000 perturbations. The distribution seems to be a power law,  $D(s) \propto s^{-\tau}$ ,  $\tau \approx 1.4$ . Figure 1b shows the distribution of durations of perturbations  $D(T)$ . This also seems to be a power law,  $D(T) \propto T^{-b}$  with  $b \approx 1.6$ . The fact that the activity does

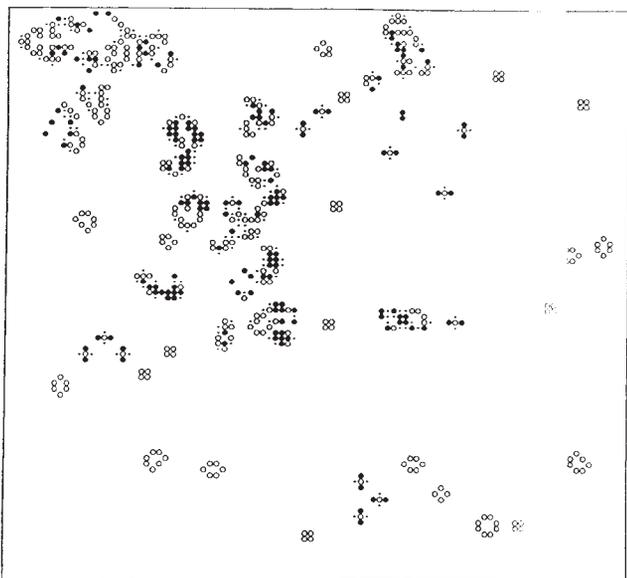


FIG. 2 Configuration of a  $100 \times 100$  system responding to a perturbation. Live passive sites are open circles, dying active sites are filled circles; the dots indicate sites where birth will take place at the next time step. Note configurations of still life (clusters of open circles), cyclic life with period 2, and propagating gliders.

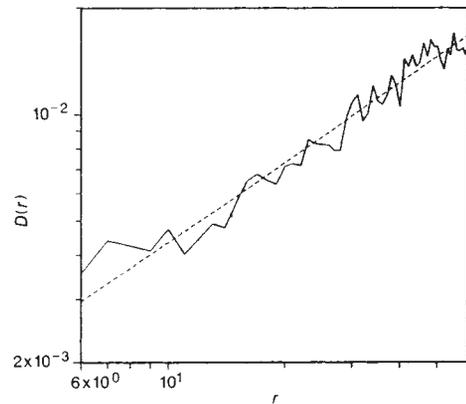


FIG. 3 Number distribution of active sites at a distance  $r$  from a given active site near the centre of a  $150 \times 150$  system.

not decay or explode exponentially (become chaotic) indicates that life and death are highly correlated in time and space: the system has evolved into a critical state. Figure 2 shows a configuration of the activity in the middle of a perturbation. Notice the clustering of the activity, which indicates that 'Life' is sustained on a fractal. The number distribution of active sites at a distance  $r$  from a given active site in an active cluster increases with  $r$  as  $D(r) \propto r^{D-1}$ , where the fractal dimension  $D \approx 1.7$  (Fig. 3). The fractal structure of the activity is not apparent in a single configuration of our rather small system, but becomes clear when averaged over many configurations. These power laws indicate that the stationary state of 'Life' is critical, with avalanches through the system on all scales. In biology, these avalanches may be thought of as the response to slow changes in the environment.

We have shown numerically that the 'Game of Life' operates at a self-organized critical state, characterized by critical exponents  $\tau$ ,  $b$ ,  $D$  and others. By analogy with traditional critical phenomena, we do not expect the critical properties to depend on the particular features of the rule, and thus they are universal. Also the model could be 'accidentally' critical, in the sense that modifications drive it away from criticality (or the model could be operating close to, but not at, the critical point so that deviations from power laws were not detected in the calculation). To check this, we have constructed a three-state model, which does not exhibit complex local configurations, but nevertheless seems to be critical, with exponents which seem to be the same as those of the 'Game of Life'<sup>8</sup>. The essential feature of the simplified model is the existence of propagating particles acting as messengers communicating between different parts of space. The simplified model is defined in any number of dimensions, and thus may be more tractable to standard renormalization-group methods known from critical phenomena. Further studies of this model may help to elucidate the critical properties of 'Life'.

The 'Game of Life' is not meant to be a realistic model for any particular system, but serves to demonstrate how large-scale structures can arise in complicated extended dynamical systems. Nevertheless, it has been suggested from studies on much more complicated mathematical models of co-evolution (S. Kauffman, personal communication) that biology indeed operates at a self-organized critical state like the one described here.  $\square$

Received 15 May; accepted 30 October 1989.

1. Berlekamp, E. R., Conway, J. H. & Guy, R. K. *Winning Ways for Your Mathematical Plays* Vol. 2 (Academic, 1982).
2. Gardner, M. *Scient. Am.* **223** (4), 120-124; (5), 118; (6), 114 (1970).
3. Bak, P., Tang, C. & Wiesenfeld, K. *Phys. Rev. Lett.* **59**, 381-384 (1987).
4. Bak, P. & Tang, C. *Phys. Today* **42**, S27 (1989).
5. Kadanoff, L. P., Nagel, S. R., Wu, L. & Zhou, S. *Phys. Rev. A* **39**, 6524-6537 (1989).

6. Bak, P. & Tang, C. *J. geophys. Res.* **95**, 15635-15637 (1989).  
 7. Carlson, J. M. & Langer, J. S. *Phys. Rev. Lett.* **62**, 2632-2635 (1989).  
 8. Chen, K. & Bak, P. *Phys. Lett.* **A140**, 299-302 (1989).  
 9. Bak, P., Chen, K. & Tang, C. *Phys. Rev. Lett.* (submitted).  
 10. Anderson, P. W. *Bull. Sante Fe Inst.* **4**, 13 (1989).  
 11. Hwa, T. & Kardar, M. *Phys. Rev. Lett.* **62**, 1813-1816 (1989).

ACKNOWLEDGEMENTS. We are grateful to L. P. Kadanoff for suggesting a few sentences for the introduction. This work was supported by the Division of Materials Science, US Department of Energy.

## Entropy of amorphous ice

Edward Whalley, D. D. Klug & Y. P. Handa

Division of Chemistry, National Research Council of Canada,  
Ottawa, Canada K1A 0R6

THE configurational entropies of amorphous solids reflect certain aspects of their structures, in particular the numbers of accessible molecular configurations. The configurational entropy of vitreous silica has been estimated theoretically<sup>1</sup> as no more than  $5.8 \text{ J K}^{-1} \text{ mol}^{-1}$ , which agrees reasonably with experiment. That of low-density amorphous ice has been estimated theoretically<sup>2</sup> as  $\sim 6.3 \text{ J K}^{-1} \text{ mol}^{-1}$  more than that of ice Ih, using a model that assumes a continuous random network of hydrogen bonds. This value corresponds to  $\sim 2.1$  more configurations per molecule than in ice Ih, and seems consistent with the result for vitreous silica<sup>1</sup>. In principle, these entropies can be obtained from the change of heat capacity from the glass to the liquid and the entropy of freezing of the liquid at equilibrium, but such measurements have not proved possible because the liquid generally crystallizes too quickly. Here we show that the entropies can be estimated approximately by another method: from the thermodynamics of the transformations of, for example, both ice Ih<sup>3</sup> and low-density amorphous ice<sup>4</sup> to high-density amorphous ice. The entropy of high-density amorphous ice relative to that of ice Ih is estimated as  $2 \pm 1 \text{ J K}^{-1} \text{ mol}^{-1}$ , and that of high-density relative to low-density amorphous ice is estimated as  $1 \pm 0.5 \text{ J K}^{-1} \text{ mol}^{-1}$ . The entropy of low-density amorphous ice relative to ice Ih is therefore  $\sim 1 \text{ J K}^{-1} \text{ mol}^{-1}$ . The earlier estimates<sup>2,5</sup> of this quantity are therefore several times too high. These low values limit the amount of disorder that can be present in the amorphous phases.

When ice Ih is compressed to  $\sim 10$  kbar at 77 K (ref. 3) it transforms to a high-density amorphous ice, several properties of which have been measured<sup>3,4,6-8</sup>. Low-density amorphous ice transforms to a high-density form in a similar way<sup>4</sup>, but at less than half the pressure at which ice Ih transforms. Both of these amorphous phases can be recovered at 77 K and ambient pressure, apparently without any significant change except for a uniform and reversible expansion<sup>3,4</sup>.

The pressure  $p_e$  at which the two phases are in equilibrium with one another is described by the equation

$$p_e = -\frac{\Delta A_e}{\Delta V_e} = -\frac{\Delta U_e}{\Delta V_e} + T_e \left( \frac{\partial p}{\partial T} \right)_e \quad (1)$$

$$\equiv p_e(1) + p_e(2), \quad (2)$$

where  $\Delta A_e$ ,  $\Delta V_e$  and  $\Delta U_e$  are the difference between the Helmholtz functions, the volumes, and the internal energies of the two phases at equilibrium, respectively,  $T_e$  is the temperature of the equilibrium,  $(\partial p/\partial T)_e$  is the slope of the equilibrium line for the two phases, and  $p_e(1) \equiv -\Delta U_e/\Delta V_e$  and  $p_e(2) \equiv T_e(\partial p/\partial T)_e$ . The difference between the enthalpies of the two phases at low pressure is the difference in the internal energy, and the internal energy changes little with pressure because it depends only on the thermal expansion and the compression. Therefore, the difference between the internal energies of the two phases under pressure can be represented, to a reasonable approximation, by the difference in enthalpy at zero pressure.

The difference between the enthalpies of high-density amorphous ice and ice Ih is  $-2,125 \text{ J mol}^{-1}$  at  $\sim 100$  K (ref. 6). As

the change of volume at the transformation of ice Ih to high-density amorphous ice is  $-4.2 \pm 0.1 \text{ cm}^3 \text{ mol}^{-1}$  (ref. 3), then, for the equilibrium between the two phases

$$p_e(1) = 5.1 \text{ kbar} \quad (3)$$

if the effect of temperature on the enthalpy changes can be neglected in a first approximation.

The contribution of the term  $T_e(\partial p/\partial T)_e$  to equation (1) is not known by direct experiment, but its range can be estimated by plotting the equilibrium pressures of ice Ih and liquid water in the range 253-273 K (ref. 9) (see curve 1, Fig. 1) and extrapolating them to low temperature. Four extrapolations have been made, assuming that the entropy change at the transformation of ice Ih to high-density amorphous ice is either 1, 2, 3 or  $6 \text{ J K}^{-1} \text{ mol}^{-1}$  and that the temperature of the glass transition at these pressures is independent of the pressure and is 150 K. This temperature is 25 K above the value measured by Klug and Handa<sup>10</sup> for low-density amorphous ice, and is the temperature at which high-density amorphous ice crystallizes when it is warmed in the range 10-30 kbar (ref. 11). The values of  $p_e(2)$  were then calculated from the temperature and the assumed slopes, and the quantities  $p_e$ , from equation (2), are plotted as the circles at 100 K in Fig. 1. The slopes of the equilibrium lines were calculated from the known volume changes at the transformations and the assumed entropy changes, and the calculated equilibrium lines are plotted in Fig. 1. The melting points at high temperatures and pressures were extrapolated in three ways to meet the slopes of the equilibrium lines for which the entropy changes at the line are 1, 2, 3 and  $6 \text{ J K}^{-1} \text{ mol}^{-1}$ . Three lines extrapolate reasonably well, and they show that the entropy of

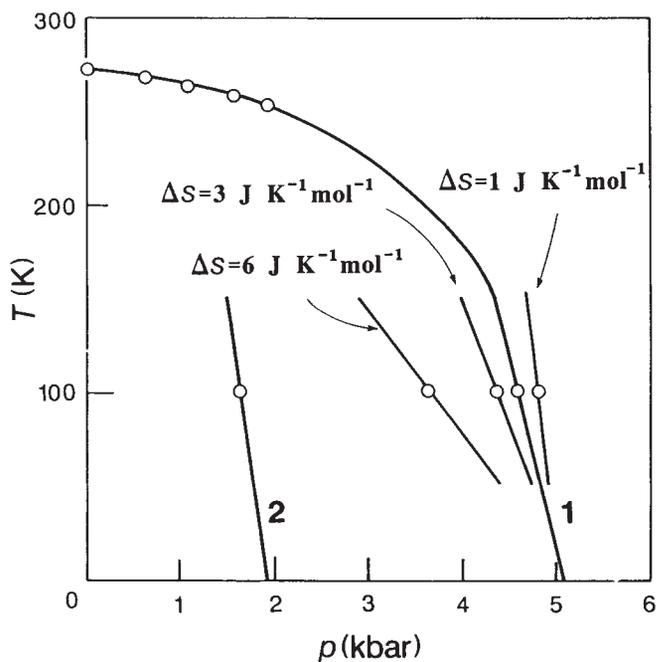


FIG. 1 Curve 1 is the equilibrium line between ice Ih and the liquid plotted in the range 0-2 kbar (ref. 9) and extrapolated to zero temperature as described in the text. Curve 2, below  $\sim 150$  K, is the equilibrium line between low-density and high-density amorphous ice, as described in the text. Curve 2 does not exist above  $\sim 150$  K because the two amorphous forms of ice melt; it is drawn only to suggest that a continuity of states might exist at low temperatures, if measurements could be made quickly enough. The equilibrium lines that would occur below the glass transition if the entropy changes at the transformation of ice Ih to high-density amorphous ice were 6, 3 and  $1 \text{ J K}^{-1} \text{ mol}^{-1}$ , are drawn through the equilibrium pressures  $p_e$  predicted by equation (1).